SASEC
1st Southern African Solar Energy Conference
21-23 May 2012

THE FLUX DISTRIBUTION FROM A 1.25M^2 TARGET ALIGNED HELIOSTAT: COMPARISON OF RAY TRACING AND EXPERIMENTAL RESULTS

Maurice Maliage[1] and Thomas H. Roos[2]

[1] Research Scientist – CSIR, P O Box 395, Pretoria, 0001, South Africa, Phone: +27-12 8413375, Fax: +27-12 3491156, E-Mail: mmaliage@csir.co.za

[2] CSIR; E-Mail: throos@csir.co.za

Abstract

The purpose of this paper is to validate SolTrace for concentrating solar investigations at CSIR by means of a test case: the comparison of the flux distribution in the focal spot of a 1.25 m^2 target aligned heliostat predicted by the ray tracing model with the experimental flux distribution measured using a calorimeter. Preliminary results show that the near-Gaussian shape and radial extent of the flux distribution in the focal spot of the 1.25m^2 heliostat is well predicted by ray-tracing simulation using SolTrace. The level of flux is underpredicted by about 50%, however. The uncertainty of the peak flux measurement was found to be between 16 and 21%, so any conclusions regarding the flux level predictive accuracy of SolTrace first require repeating the experimental measurements taking care to increase the sensitivity of the flux measurement.

Keywords: Ray tracing, SolTrace, Heliostat, Beam down mirror, Calorimeter

1. Introduction

The development of concentrating solar technologies require the ability to model optical processes with a high degree of fidelity, to enable trade-offs to be evaluated before committing to expensive experimentation. The availability of free ray tracing software such as SolTrace from NREL potentially reduces the barrier to entry for concentrating solar power researchers by removing the license fees payable for proprietary software. Before such software can be used with confidence, however, validation against experimental test cases of suitable resolution is required. This paper describes the generation of a numerical model in Soltrace of the experimental setup, to allow evaluation of the predictive capability of Soltrace.

2. Description of experiment

The test case used is extensively described by Roos et al [1], but will be briefly summarized here. The experiment was performed in July 2011 between buildings 11 and 12 at CSIR. A 1.25 m^2 target-aligned heliostat was used to generate a solar focal spot. Instead of a spherical mirror, use is made of twelve 300mm × 300mm flat mirror panels (providing 1.08m^2 of reflective area), in three columns and four rows, canted to produce a single focal spot at a focal distance of about 50m. A 1.0m × 1.5m flat beam-down mirror reflects the focal spot downward into a cold water calorimeter, comprising a hollow hemispherical cavity with entrance aperture diameter of 0.85m, internally lined with 11 discrete copper coils, internally cooled by adjustable water flowrates. The inlet and outlet water temperatures are measured using PT100 RTDs thermocouples and the water flowrates with paddle-wheel flowmeters. The copper coils are painted with a highly absorptive (96.25%) coating. The flux is therefore determined from the temperature rise of the water and the massflow. The 11 separate copper coils allow a radial distribution of the heat flux to be determined.

3. Description of SolTrace

SolTrace is a Monte-Carlo ray-tracing software package downloadable from the website of the National Renewable Energy Laboratory (NREL) [2]. It runs on both Windows and Mac OS X systems. The theory used is that of Spencer and Murty [3].

Figure 1 shows a screenshot from a SolTrace simulation. On the far left are icons to open windows for different stages in the creation and execution of a ray-tracing simulation:

- Sunshape definition
- Optical properties of material
- Geometrical information of different stages
- Ray-trace options
- Results

On the right is a view of a three-dimensional ray tracing simulation. The positive y-direction is vertical, the positive x-direction is due east and the view into the page is due north. Individual rays (yellow lines) are shown, traced downward from the sun (at approximately 45°), reflecting off the mini heliostat panels (bottom right of white grid) upward to beam-down mirror (top left of grid), and finally reflected vertically downward into the calorimeter.

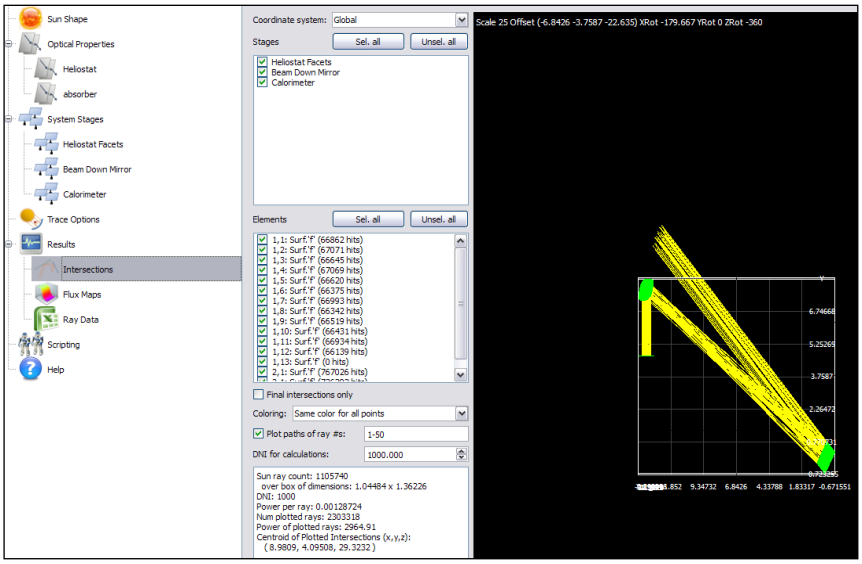

Figure 1: Screenshot showing the ray tracing simulation results and the stages in SolTrace

4. Development of SolTrace model

The SolTrace model definition and run execution comprises several steps, such as definition of sun shape, optical properties and system stages which define the ray tracing model. Each of these levels is explained in the section below.

4.1. Sun shape and position

Unfortunately, the latitude, day and hour calculator appears not to work in the Southern hemisphere, so the position of the sun must be manually defined in terms of the X, Y and Z components of the solar unit vector in global coordinates (see Figure 2).

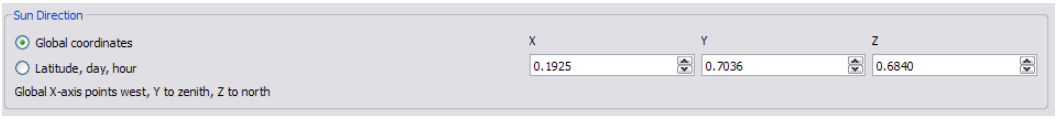

Figure 2. Screenshot showing the sun direction defined in the X, Y and Z global coordinates

The general expression to determine the sun direction in terms of the X, Y and Z components of the solar unit vector is given below. In this case the X-axis points west, Y to zenith, Z to north and the sun direction equation is

$$\hat{s} = [x_s, y_s, z_s]$$

$x_s, y_s$and $z_s$are given conventional solar azimuth and elevation and are also define as

$$x_s = -cos(\, s_{el}\,) \sin(s_{az})$$

$$y_s = \sin(s_{el})$$

$$z_s = \cos(s_{el}) \cos(s_{az})$$

where s_{el} denote solar elevation and s_{az} solar azimuth. A useful solar position website [4] was used to find the solar elevation and azimuth angles relative the heliostat as a function of latitude, longitude, date and time of the day. The above equations were entered into a Microsoft Excel spreadsheet (see Table 1), and used to convert the solar elevation and azimuth angles to a solar unit vector which was then entered into the dialog box shown in Figure 2.

Various options to define sun shape profiles are provided in SolTrace, such as such as pillbox, Gaussian and user-defined profles. The pillbox and Gaussian sun shapes were selected as shown in Figure 3 and utilized in separate simulations in order to identify any changes in the peak flux distributions (see section 5). Both simulations were performed using the same desired number of ray intersections.

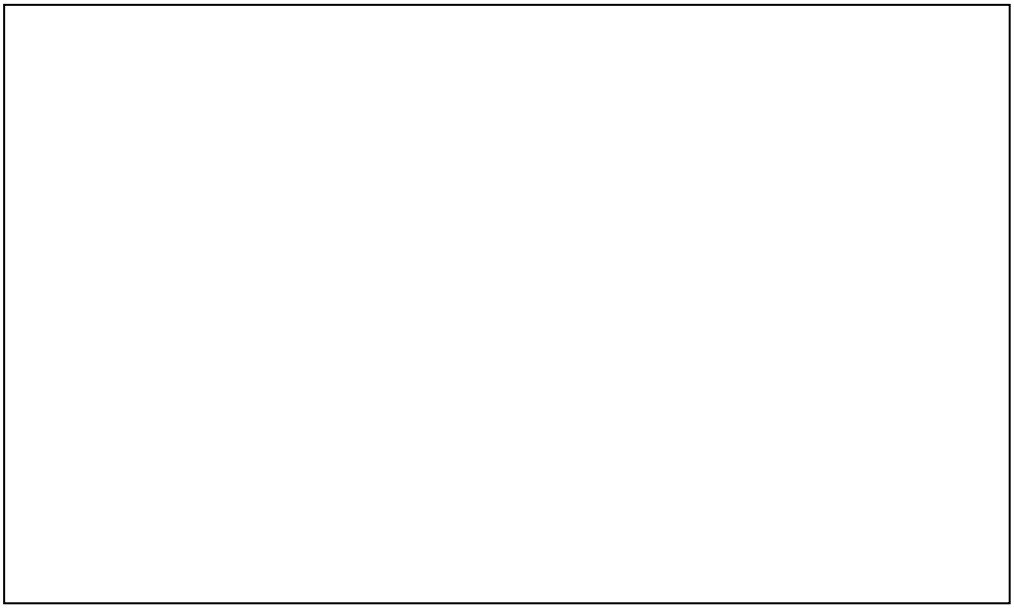

Figure 3. Screenshot shows the pillbox and gaussian sunshapes

As DNI had not been measured during the experiment (due the equipment being off-site for a separate

project), a value of 1000W/m^2 was assumed for the ray-tracing simulation.

4.2. Optical properties of the reflecting material

A dialog box requires the various optical properties to be entered. In this case the reflecting material (mirror) is assumed to have a reflectivity of 0.82 and transmissivity of 1 as shown in Figure 4. For optical properties such as slope error, specularity error, error type, refraction index and others default values were taken. The reflectivity of the calorimeter surface was set to 0.0375.

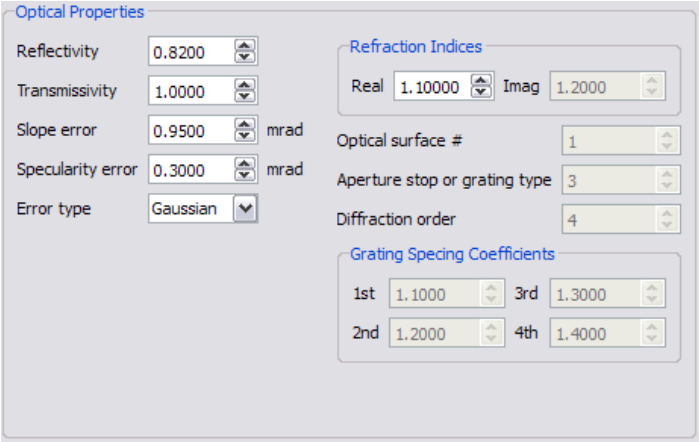

Figure 4.Screenshot shows optical properities based on the reflecting material (mirror)

4.3 System stages

4.3.1 Geometries

The first step in creating the stages was to generate a CAD model of the experimental setup, in order to generate and define the position and orientation of all reflecting panels which need to be described as input parameters in the ray tracing simulation. The definitions of the stages labeled in the CAD model as shown Figure 5 are as follows:

- The mini-heliostat is a small scale research instrument that uses a mirror to reflect the sun rays towards a predetermined target.
- The beam down mirror (target) is a physical object, distant from the heliostat and is stationary relative to the heliostat. It reflects the sun's rays from the heliostat towards the calorimeter
- The calorimeter is a device used to measure the concentrated solar flux distribution

This required taking physical measurements of all the dimensions of, and distances between, the heliostat, buildings involved, the beam-down mirror and the calorimeter. Figure 5 shows a view of the resultant Solidworks CAD model generated.

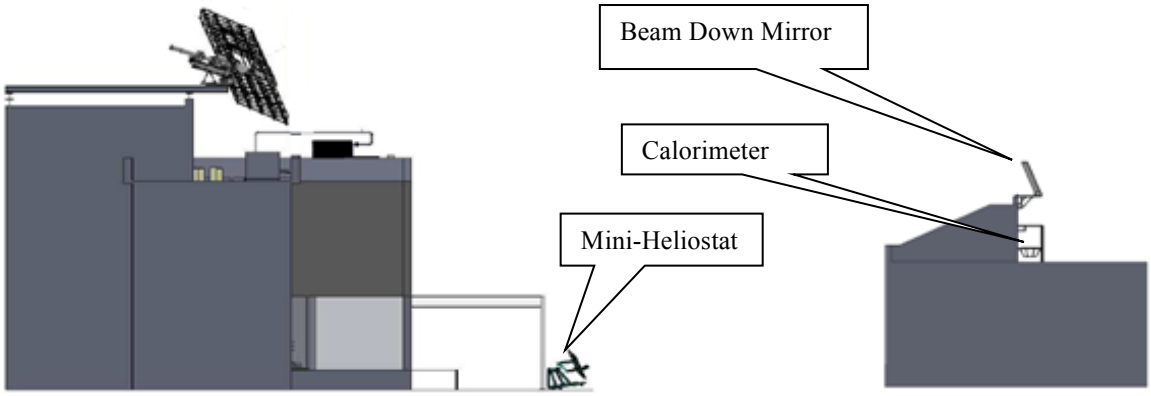

Figure 5: A CAD model of support building to determine orientation of all reflecting planes and target

The second step was to define all the reflecting surfaces in SolTrace, with the relevant data at the appropriate stage. The experimental setup is a three-stage system.

The first stage is the target-aligned heliostat. The mirror panel positions of the heliostat are defined in terms of the heliostat coordinate system, centered in the centre of the mirror array. The x- and y-axes lie in the plane of the mirror array, where the x-axis coincides with the pitch or "elevation" axis of the heliostat. The z-axis is normal to the mirror array.

The second stage is the beam down mirror, with positional coordinates relative to the heliostat obtained by means of the Solidworks CAD model. The third stage is the calorimeter, positioned relative to the beam down mirror. For the purposes of the SolTrace model, the hemispherical calorimeter is represented by a circular flat plane of 0.85 m diameter at the calorimeter entrance.

4.3.2 Aiming points and surface normals

The CAD model was also used to obtain the correct surface normals to ensure incident and reflected rays are correctly aligned. Once all the position and orientation adjustments had been made to the heliostat mirror panels and beam down mirror, the SolTrace model was ready to run the ray tracing simulation.

The normals from the different stages then needed to be defined relative to each other. The target position relative to the heliostat was used to obtain the target unit vector. This, together with the solar unit vector, was used to generate the heliostat normal unit vector.

Solar Elevation (Degree)	44.72		
Solar Azimuth (Degrees)	344.28		
Coordinates	X	Y	Z
Solar Unit Vector ($\hat{s}$)	0.192515	0.70364278	0.683977216
Target Coordinates	13.75976	7.75590000	44.92788000
Target Unit Vector ($\hat{t}$)	0.288928	0.16285861	0.943396934
Heliostat Normal Unit Vector ($\hat{n}$)	0.252659	0.45473525	0.85403717

Table 1. The X, Y and Z coordinates for the solar unit vector, target unit vector and heliostat normal unit vector.

The x, y and z components of the heliostat aiming point unit vector was obtained using the Microsoft Excel spreadsheet (see Table 1), as explained in the previous section and inserted in the ray tracing model as shown

in Figure 6. This is a very significant part of the ray tracing simulation model since if the aiming point is wrongly defined, the beam from the heliostat will miss the target. The general expression used in determining the heliostat aiming point was defined as the normal vectors in terms of the target and the sun vector as follows

$$\hat{n} = \frac{\hat{s} + \hat{t}}{\sqrt{2(1 + \hat{s}.\hat{t})}}$$

$\hat{n}$, $\hat{s}$ and $\hat{t}$ are the heliostat unit vectors, solar unit vector and target unit vector respectively. The beam down mirror aiming point was obtained as a function of the target coordinates.

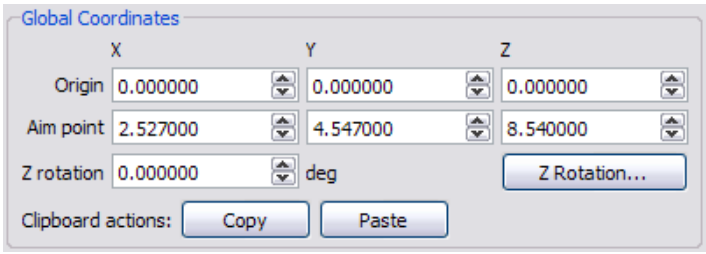

Figure 6. Screenshot shows the heliostat aiming point within the global coordinate system

4.3.3. Astigmatism Correction

The standard mirror canting approach used by SolTrace is spherical, and use is made of an "aim point", which is in effect the point at which the normals of the mirror surfaces converge. Adjustments can be made to the "aim points" of individual mirror panels. This option was used to increase the effective radius of curvature in the sagittal plane by diverging the y-axis aimpoints (in the coordinate system of the heliostat). At non-zero incidence angles this has the effect of bringing the individual focal spots of mirror panels at different distances from the heliostat pitch axis together. The original divergence of these focal spots was caused by the astigmatism which occurs at non-zero incidence angles. This is the numerical equivalent of the experimental "off-axis canting" which was done on the heliostat.

5. Ray-Tracing Results

5.1. Discussion

A comparison of the experimental test results and the ray tracing simulation result are presented in Figure 7.

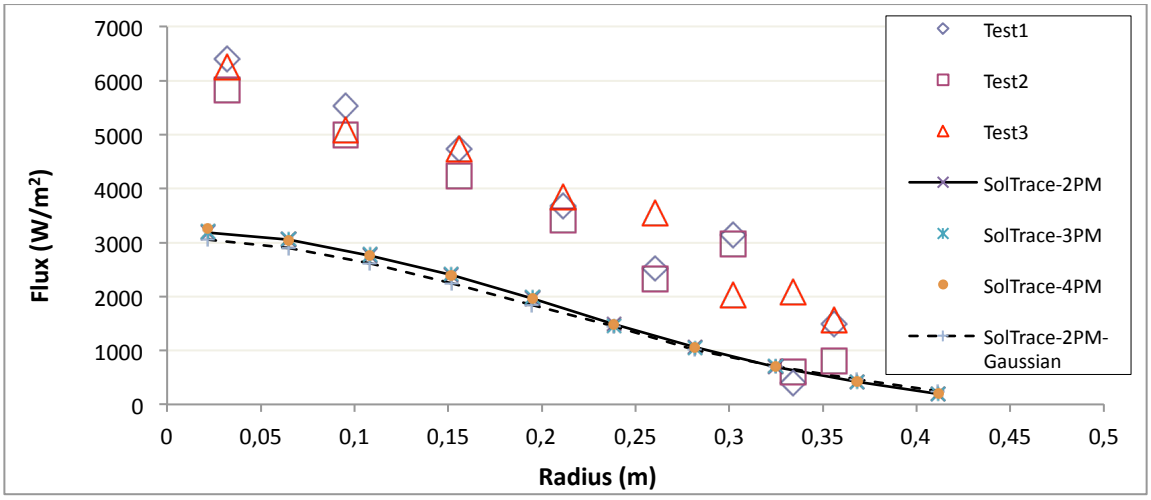

Figure 7.: Comparison of measured and predicted flux distributions

The radial extent of the heliostat focal spot appears to be relatively well predicted, with ray-tracing predictions agreeing with experimental flux levels at a radius of about 0.35m. The shape of the flux distribution also appears to be well captured, resembling a Gaussian distribution. The peak flux levels are underpredicted by about 50%, however.

5.2. Ray tracing parameter variation

The discrepancy could possibly be explained by ray-tracing underprediction. Different approaches were followed to explore the discrepancy. Firstly, the fact that the experimental values exceed the ray-tracing values excludes incorrect ray-tracing DNI as the cause, as 1000W/m^2 is an optimistic value for the location. Secondly, the time of day for the ray-tracing simulation was varied from 14:00 to 16:00. Figure 8 shows the effect in terms of incident angle of the rays (the view direction is the same as Figure 1): the first screen shot shows the orientation of the sun at 14:00, the second at 15:00 and the third at 16:00.

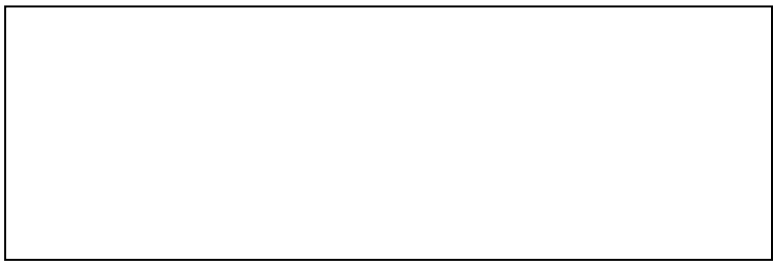

Figure 8. Screenshot shows orientation of the sun as a function of solar elevation and azimuth angle

Thirddly, the sunshape used in the simulation was varied, with a single simulation performed for 14:00 using a Gaussian rather than pillbox sunshape as shown in Figure 3. As can be seen in Figure 7, the differences induced by these two modifications are not significant, and do not explain the discrepancy.

5.3. Sensitivity of experimental apparatus

The discrepancy could alternatively possibly be explained by experimental over-reading. The calorimeter had been designed for use with the much larger 25 m^2 target-aligned heliostat, visible in the top left corner of Figure 5. The measured heat transfer is

$$\dot{q} = \dot{m}c_p\left(T_{out} - T_{in}\right) = \dot{m}c_p\Delta T$$

Systematically over-reading heat transfer may be due to overreading the water flowrate $\dot{m}$, the outlet water temperature T_{out} or under-reading the inlet water temperature T_{in}. There are 11 flowmeters and outlet RTD's but only one inlet water RTD. The RTD's were not specially calibrated, but their factory calibrations were used. Applying uncertainty analysis principles:

$$\therefore (\delta\dot{q})^2 = \left(\frac{\partial\dot{q}}{\partial\dot{m}}\right)^2(\delta\dot{m})^2 + \left(\frac{\partial\dot{q}}{\partial c_p}\right)^2(\delta c_p)^2 + \left(\frac{\partial\dot{q}}{\partial T_{out}}\right)^2(\delta T_{out})^2 + \left(\frac{\partial\dot{q}}{\partial T_{in}}\right)^2(\delta T_{in})^2$$

$$\therefore \frac{\delta\dot{q}}{\dot{q}} = \sqrt{\left(\frac{\delta\dot{m}}{\dot{m}}\right)^2 + \left(\frac{\delta T_{out}}{(T_{out} - T_{in})}\right)^2 + \left(\frac{\delta T_{in}}{(T_{out} - T_{in})}\right)^2}$$

The absolute massflow measurement uncertainty of the Bürkert Instruments *low-flow wing wheel* 8081 model flowmeters used is 0.01% of the full scale value of 0.333kg/s, or 0.0001 × 0.333kg/s = 3.33 × 10^{-5} kg/s. The absolute temperature measurement uncertainty for the WIKA Instruments Class B PT100 RTDs (1/10 DIN) chosen are ±0.04ºC at 20ºC and ±0.05ºC at 40ºC. For the design condition of 80 suns from the 25m^2

heliostat, flowrates in the 11 tubes of the calorimeter range from 0.02kg/s to 0.15kg/s, and the tube temperature difference (from inlet to outlet) is 10ºC. The design heat flux uncertainty is

$$\therefore \frac{\delta \dot{q}}{\dot{q}} = \sqrt{\left(\frac{\delta \dot{m}}{\dot{m}}\right)^2 + \left(\frac{\delta T_{out}}{(T_{out} - T_{in})}\right)^2 + \left(\frac{\delta T_{in}}{(T_{out} - T_{in})}\right)^2} = \sqrt{\left(\frac{3.33e-5}{0.02}\right)^2 + \left(\frac{0.04}{10}\right)^2 + \left(\frac{0.05}{10}\right)^2} = 0.00661 < 1\%$$

When applied to the much smaller 1.25 m^2 target-aligned heliostat, the picture changes. From Table 2 it can be seen that for the first 8 tubes in tests 1 to 3 of this experiment (see Figure 7), the flowrates vary from 0.00070 to 0.044, the temperature differences across the tubes from 0.213ºC to 4.463ºC and the calculated uncertainties of heat flux from 3.1% to 30.1%.

Test	Property	Tube number							
		1	2	3	4	5	6	7	8
1	ΔT (ºC)	0.354	0.572	0.276	0.336	0.228	0.294	1.450	2.259
	Flowrate (kg/s)	0.0154	0.0223	0.0407	0.0439	0.0423	0.0279	0.0007	0.0018
	Flux Uncertainty (%)	18.1	11.2	23.2	19.0	28.1	21.8	6.5	3.4
2	ΔT (ºC)	0.309	0.537	0.245	0.310	0.213	0.267	1.407	2.342
	Flowrate (kg/s)	0.0160	0.0214	0.0408	0.0440	0.0419	0.0291	0.0009	0.0013
	Flux Uncertainty (%)	20.8	11.9	26.2	20.6	30.1	24.0	5.5	4.5
3	ΔT (ºC)	0.388	0.619	0.321	0.398	0.534	4.463	3.601	3.917
	Flowrate (kg/s)	0.0138	0.0189	0.0350	0.0387	0.0253	0.0012	0.0015	0.0011
	Flux Uncertainty (%)	16.5	10.3	19.9	16.1	12.0	3.1	2.9	3.5

Table 2. Experimental □T, flowrates and resultant flux uncertainties for each of the calorimeter tubes

The uncertainties of tube 1 (which measures the peak fluxat the centre of the calorimeter) can be seen to vary from 16.5 to 20.8%. While significant, this can account for at most some 2/5^{ths} of the 50% discrepancy seen between the ray tracing and experimental results.

It can also be seen that test 3 attains lower uncertainties than the other two tests, by having lower flowrates and therefore higher temperature differences. If during the experiment the flowrates had been halved, the temperature rise across each of the pipes can be expected to have doubled for the same heat flux levels. It appears that near-minimum uncertainties would have been reached had the flowrates been reduced by a factor of about 10. The results of a manual tube-by-tube flowrate optimization are shown in Table 3. It can be seen that best results are obtained for tubes 1-6 at flowrates between 0.0016 and 0.0030 and at tube temperature rises between 3ºC and 5.5ºC.

Test	Property	Tube number							
		1	2	3	4	5	6	7	8
1	ΔT (ºC)	3.186	5.153	4.695	5.382	4.329	4.112	1.450	2.801
	Flowrate (kg/s)	0.0017	0.0025	0.0024	0.0027	0.0022	0.0020	0.0007	0.0015
	Flux Uncertainty (%)	2.80	1.83	1.95	1.67	2.10	2.28	6.48	3.24
2	ΔT (ºC)	3.085	4.832	4.406	5.278	4.043	3.740	1.731	1.874

	Flowrate (kg/s)	0.0016	0.0024	0.0023	0.0026	0.0022	0.0021	0.0009	0.0012
	Flux Uncertainty (%)	2.94	1.93	2.07	1.77	2.19	2.34	5.27	4.45
3	ΔT (ºC)	3.102	4.955	4.500	5.171	5.340	3.124	3.241	2.742
	Flowrate (kg/s)	0.0017	0.0024	0.0025	0.0030	0.0025	0.0017	0.0016	0.0016
	Flux Uncertainty (%)	2.83	1.91	1.95	1.67	1.78	2.84	2.83	3.17

Table 3. Optimum □T and flowrates for minimum resultant flux uncertainties

6. Conclusion

An available concentrating solar flux dataset was used as a test case for the NREL SolTrace ray-tracing software. The shape of the flux distribution and the angular spread of the resultant focal spot appeared to be relatively well predicted, but the peak flux intensity was underpredicted by 50%. After investigation it became clear that during the experiment the calorimeter flowrates were too high by a factor of about ten, resulting in low temperature rises with correspondingly higher relative temperature measurement uncertainty and therefore between 16.5 and 20.8% flux uncertainty. Conclusions regarding the predictive accuracy of SolTrace therefore require further work, including calibrating the RTD's (taking care regarding the inlet flow RTD) and not using the factory calibration, repeating the experimental tests at flowrates approximately 1/10th of those of the previous test run, and simultaneously measuring DNI.

Acknowledgements

The authors would like to thank CSIR R&D office for directly supporting this work.

References

[1] Roos, T.H., Du Plessis, G., Klein, P., Bode, S., and Landman, W., (2011), "The Manufacture and Preliminary Testing of a Cold Water Calorimeter for Use With and Without a CPC", Presented at SolarPaces2011, Granada, Spain, September 2011

[2] http://www.nrel.gov/csp/soltrace/download.htm (accessed 24 August 2011)

[3] Spencer, G.H., and Murty, M.V.R.K., (1962), "General Ray-Tracing Procedure," Journal of the Optical Society of America, Vol, 52, June, pp.672-678.

[4] http://www.esrl.noaa.gov/gmd/grad/solcalc/ (accessed 5 March 2012)